Collapse of the EPR fine structure of a one-dimensional array of weakly interacting binuclear units: A dimensional quantum phase transition

Rafael Calvo,[1,*] Julián E. Abud,[1] Rosana P. Sartoris,[1] and Ricardo C. Santana[2]

[1]*Departamento de Física, Facultad de Bioquímica y Ciencias Biológicas and INTEC, CONICET-Universidad Nacional del Litoral, Güemes 3450, 3000 Santa Fe, Argentina*

[2]*Instituto de Física, Universidade Federal de Goiás, Campus Samambaia, CP 131, 74001-970 Goiânia (GO), Brazil*

(Received 20 May 2011; revised manuscript received 18 July 2011; published 19 September 2011)

Binuclear (also called dimeric) compounds with pairs of antiferromagnetically coupled spins $\frac{1}{2}$, $\mathbf{S_1}$ and $\mathbf{S_2}$ ($H_{ex} = -J_0\ \mathbf{S_1}.\mathbf{S_2}$, with $J_0 < 0$ for antiferromagnets), have been around for ∼60 years, providing roots to the field of molecular magnetism. In addition, as reported in recent years, weak interactions between binuclear units in a crystalline network give rise to interesting systems of interacting bosons having an energy gap, which are important in the study of quantum phenomena in many body systems coupled by stochastic distributions of interactions. Binuclear compounds have gained new relevance in the last decade with the observation of Bose-Einstein condensation. In this work, we use electron paramagnetic resonance (EPR) to study the role of weak inter-binuclear exchange couplings J' ($|J'| \ll |J_0|$) in the spectra, elementary excitations, and spin dynamics of a one-dimensional (1-D) array of antiferromagnetic (AFM) binuclear units in the hybrid (organic-inorganic) Cu^{II} compound $[Cu(CH_3COO)(phen)(H_2O)]_2{\cdot}(NO_3)_2{\cdot}4H_2O$. In this material, the acetate $(CH_3COO)^-$ anion supports the intra-binuclear exchange coupling J_0, and the stacking of the (phen) = 1,10-phenanthroline rings of neighbor units supports the inter-binuclear interactions J', giving rise to well-isolated chains. This has advantages over other binuclear compounds studied previously because magnetically equal units are arranged in a 1-D spatial arrangement along the direction of their symmetry axis, simplifying the analysis of the data and allowing a simpler treatment. In addition, single crystals of good quality allow detailed EPR experiments.

EPR spectra were collected at ∼33.8 and ∼9.4–9.8 GHz in oriented single crystals at room temperature and in powder samples at temperatures (T) between 10 and 300 K. By varying the energy levels of the binuclear units with the magnetic field orientation, or changing the population of the excited triplet state with temperature and, consequently, the effective coupling between units, we observe in single-crystal samples sudden merges of the fine structure peaks, accompanied by a large narrowing, when the inter-binuclear coupling becomes larger than the splitting of the triplet state. In addition, and because of this collapse of the fine structure peaks, the spectra of powder samples display a strong and unexpected central peak that decreases in intensity with decreasing temperature, as it occurs with the binuclear signals. We first discuss the dimensional quantum phase transition indicated by the spectral changes using Anderson-Kubo's theory of exchange narrowing. The data allow evaluation of the binuclear exchange coupling $J_0 = (-74 \pm 3)\ cm^{-1}$, and the interactions between neighbor binuclear units $|J'| = (0.04 \pm 0.01)\ cm^{-1}$. We also consider the magnetic excitations (triplet excitons or triplons) arising from the inter-binuclear couplings, and introduce a model explaining qualitatively the observed collapse and narrowing of the EPR spectra in terms of these excitons. We analyze the role of temperature in the inter-binuclear interactions and the exchange correlation times of the binuclear systems and compare our results with those in binuclear compounds in which Bose-Einstein condensation occurs.

DOI: 10.1103/PhysRevB.84.104433 PACS number(s): 75.10.Jm, 75.40.Cx, 75.40.Gb, 76.30.−v

I. INTRODUCTION

Since Bleaney and Bowers[1] explained their electron paramagnetic resonance (EPR) results and the magnetic susceptibility data reported by Guha[2] for antiferromagnetic (AFM) copper acetate monohydrate, binuclear units (also called "dimeric units") of ions with unpaired spins have been extensively studied. Impressive numbers of investigations with different perspectives have been reported by physicists, chemists, and biologists, and reviewed in books and articles.[3–9] New questions, and new experimental and theoretical answers have kept interest in the problem alive along the years. The best-known binuclear compounds contain Cu^{II} ions, but many contain other 3d or 4f ions,[6,10,11] or alternate units of 3d and 4f ions,[12] with inorganic, organic, or hybrid (organic and inorganic) ligands.

An AFM binuclear unit α has two spins $\frac{1}{2}$, $\mathbf{S_{1\alpha}}$ and $\mathbf{S_{2\alpha}}$, coupled by an isotropic exchange,

$$H_{ex}(\alpha) = -J_0\ \mathbf{S_{1\alpha}} \cdot \mathbf{S_{2\alpha}}, \tag{1}$$

where $J_0 < 0$.[6] It has a singlet nonmagnetic ground state (S = 0), and an excited triplet state (S = 1) at an energy $|J_0|$, for which the EPR spectrum and magnetic behavior are well understood. Since the singlet ground state $\varphi_0(\alpha)$ (S = 0) is nonmagnetic, the magnetic response of AFM binuclear units arises from the thermally populated excited state S = 1. A binuclear material containing interacting identical units in a field $\boldsymbol{B_0} = \mu_0 \boldsymbol{H}$ (μ_0 is the permeability of the vacuum) is

described by:

$$H = \sum_{\alpha}[-J_0\,\mathbf{S_{1\alpha}}\cdot\mathbf{S_{2\alpha}} + \mathbf{S_{1\alpha}}\cdot\boldsymbol{D_{12}}\cdot\mathbf{S_{2\alpha}} + \mu_B(\mathbf{S_{1\alpha}}\cdot\boldsymbol{g_1} + \mathbf{S_{2\alpha}}\cdot\boldsymbol{g_2}).B_0] - \sum_{i,j,\alpha\neq\beta} J'_{i\alpha,j\beta}\mathbf{S_{i\alpha}}\cdot\mathbf{S_{j\beta}}, \quad (2)$$

where the traceless spin-spin interaction matrix $\boldsymbol{D_{12}}$ considers anisotropic spin-spin couplings (dipole-dipole or anisotropic exchange) within the excited spin triplet, and, in the cases of interest, it is $|\boldsymbol{D_{12}}| \ll |J_0|$. Equation (2) neglects the usually small anisotropic spin-spin couplings between spins in neighbor units. The third term is the Zeeman coupling, where $\boldsymbol{g_1}$ and $\boldsymbol{g_2}$ are the g-matrices (which may be different, equal, or symmetry related), and μ_B is the Bohr magneton. $J'_{i\alpha;j\beta}$ represents the exchange couplings between spins i and j in neighbor binuclear units α and β in the triplet state, giving rise to a random distribution of couplings between a unit and the environment of units. In our case (see the structural description), we consider equal couplings J' with only two neighbor units in a chain array. Noninteracting (isolated) binuclear units have $|J'| = 0$, zero magnetic dimension, and a limiting ground state wave function,

$$\Psi_0 = \prod_{\alpha}\varphi_0(\alpha),$$

is approached when the temperature $T \to 0$ and the thermal population of the excited triplet state, $\rho \propto \exp(-|J_0|/k_BT)$, decreases. As T increases and the triplet state becomes populated, the interactions J' give rise to the dynamics of the thermally excited units in the triplet state, which may be described in terms of the S = 1 "triplet excitons" or "triplons,"[13] as introduced by Overhauser[14] to explain multiplet structures occurring in the optical spectra of ionic crystals, and which were applied ~50 years ago to investigate the EPR spectra of molecular crystals and solid free radicals.[15–17] In 1990, Sachdev and Bhatt introduced a representation of S = $\frac{1}{2}$ quantum spins that is useful to describe the transition between dimerized and magnetically ordered quantum antiferromagnets.[18] Other authors have treated the problem with related objectives.[9,19,20]

The discovery of high-T superconductors stimulated interest in low-dimensional interacting spin systems (quantum many-particle systems), which provide information about elementary excitations,[9,17,18,21,22] quantum phase transitions,[23] and critical phenomena.[23,24] Also, the efforts of many physicists were triggered by the fact that AFM binuclear magnetic materials having an energy gap are well fitted to display Bose-Einstein condensation[19,25,26] at relatively high T.[9,26,27] Chemists are more interested in the correlations between exchange couplings and bond structure in binuclear and polynuclear units, and in the design of new bonds for new molecular magnetic materials.[6,28] The phenomena investigated and the methods used by physicists and chemists are different, and this divergence (and fruitful complementarity) has become stronger over the last ~10 years.

In order to investigate systems having an energy gap in the absence of B_0,[23,27] inorganic binuclear materials as $TlCuCl_3$[9,21,25,26,29,30] and $BaCuSi_2O_6$[31–35] have been studied as a function of B_0, T, and hydrostatic pressure, particularly for $B_0 \sim |J_0|/(g\mu_B)$ when the ground state changes to a magnetic state. Inelastic neutron diffraction experiments have provided important achievements related to Bose-Einstein condensation,[9] and the triplons have been invoked to explain the collective behavior observed in the experiments.[29]

In paramagnetic solids (e.g., weakly interacting identical spins $\frac{1}{2}$), the isotropic exchange interactions do not produce a direct effect on the EPR spectra because they commute with the total spin, and consequently with the Zeeman Hamiltonian operator. However, they generate spin dynamics that average out the effects of anisotropic spin-spin interactions (e.g., dipole-dipole interaction), thus narrowing the line and changing the spectra. This *exchange narrowing* phenomenon was proposed by Gorter and Van Vleck,[36] and explained mathematically by Van Vleck[37] using the moment method. Anderson[38,39] advanced over these ideas with a theory emphasizing the stochastic nature and the dynamics of the interactions between spins, and allowing the spectrum to be computed in terms of the energy-level scheme of the individual spins, and the magnitudes and distribution of interactions. Kubo and Tomita[40–42] treated the problem with equivalent results using statistical mechanics. As in thermodynamic problems where the particles are assumed to interact with a thermal bath, in the exchange narrowing theory, a spin system is characterized as individual spins interacting with a *spin bath*, through exchange and dipolar interactions. For weakly coupled paramagnetic systems (with no energy gap), this spin-bath has in general no thermal activation, which imposes particular characteristics onto the interaction and equilibrium conditions.[43] Elementary excitations provide a complementary view of this problem.

Within a line of research about very weak exchange interactions supported by long and not covalent chemical paths, we and others[44–46] observed abrupt transitions in the EPR spectra of weakly coupled anisotropic paramagnetic spin systems when the energy levels of the spins were varied with the magnetic field orientation. In these quantum phase transitions, the systems evolve between localized and collective (extended) spin states as consequence of the stochastic distributions of exchange couplings between a spin and the spin bath. The spectral peaks corresponding to magnetically different ions merge to a central position when the magnitude of the T-independent root mean square (rms) average interaction between a spin and its neighbors equals the relevant energy differences,[38,39] and the split and collapsed quantum states differ in the localization and dimensionality of the wave function.[46] Phase transitions with similar characteristics occur in a wide group of unrelated physical problems[47] and are relevant to the study of spin decoherence processes, contributing new and relevant information to the fields of quantum information and quantum computers. From the experiments in paramagnetic materials, small average exchange couplings between the individual spins and the spin bath (e.g., $|J'| \sim 0.005$ cm^{-1}, where 1 cm^{-1} = 0.124 meV = 2.9979 × 10^4 MHz) were evaluated at room T, even in the presence of much larger exchange interactions.[44,45] Evaluating extremely weak exchange couplings,[46] is useful to estimate matrix elements for electron transfer in model compounds for biological molecules,[48] and to study the coupling between polynuclear spin systems in molecular magnets.[49]

Bleaney and Bowers[1] and many others[4–8,11,33–35,50–56] have used EPR to investigate binuclear units. The technique allows the properties of the triplet state to be studied, measuring the coupling J_0 Eq. (1), and estimating the interactions J' between units Eq. (2), even without having data at low T or high magnetic fields. In recent years, we studied powder and single-crystal samples of materials containing weakly coupled AFM binuclear units[53,54] and, as for the case of weakly coupled paramagnetic spins, observed that the positions and widths of the signals display abrupt phase transitions between localized and collective spin states. This is produced by changing the positions of the energy levels with the magnetic field direction,[53] or varying the average coupling with the spin bath, changing with T the population of the triplet state.[54] The fact that AFM binuclear compounds allow Bose-Einstein condensation transitions stimulated us to do further research in the subject. The possibility of following the thermal activation of the spin bath and the correlation times of the spin dynamics of binuclear units with thermally accessible excited states adds interesting ingredients to this problem.

Here, we use EPR at ∼33.8 and ∼9.4–9.8 GHz to study powder and single-crystal samples of the AFM hybrid (organic-inorganic) binuclear compounds $[Cu(CH_3COO)(phen)(H_2O)]_2{\cdot}(NO_3)_2{\cdot}4H_2O$, where the acetate $(CH_3COO)^-$ anions bridge the copper atoms in the binuclear molecules, supporting the exchange coupling J_0, and the stacking of the (phen) = 1,10-phenanthroline ligands supports the couplings J' between neighbor binuclear units along one direction. This 1-D magnetic dimensionality should show up in the spin dynamics of the compound.[53,54] It will be called $Cu_2ac_2phen_2$, and its structure and magnetic susceptibilities were reported by Tokii *et al.*[57] According to the susceptibility measurements,[57] it has $J_0 = (-86 \pm 3)$ cm^{-1} (equal to −10.7 meV). The structure is monoclinic, with all magnetically identical binuclear units, simplifying the experiments and the interpretation of the data.

$Cu_2ac_2phen_2$ has similarities and differences with binuclear $TlCuCl_3$ and $BaCuSi_2O_6$. The energy gap $|J_0|$ is larger, and the ratio $|J'/J_0|$ is ∼3 orders of magnitude smaller. Our results allow the merging of the fine structure peaks of the excited spin triplet of the units to be followed as a function of the magnitude and orientation of the magnetic field, and as a function of the average interaction between an isolated unit and the T-dependent spin bath. We observe wider ranges of variation of the spectra, and larger changes of the energy-level structure than in previous works, following in detail a quantum phase transition related to the localization and dimensionality of the binuclear units.

We describe first the experimental procedures and the structure of the compound.[57] Later, we describe and analyze the data using Anderson-Kubo's theory and also considering the spinned elementary excitations arising from the inter-binuclear coupling, and we compare our results with those obtained in other materials having interacting binuclear units. A conclusions section summarizes the results of our work.

II. EXPERIMENTAL PROCEDURES

A. Sample preparation

Samples of $Cu_2ac_2phen_2$ were prepared as reported by Tokii *et al.*[57] and identified by powder x-ray diffraction. Single crystals, each having ∼1 mm along each direction and displaying well-formed ac planes and the $\boldsymbol{c}$-axis, were glued on cubic sample holders obtained by cleavage of large single crystals of KCl. These holders were used as "laboratory systems of coordinates" to orient the samples, with the $\boldsymbol{a}^* = \boldsymbol{b} \times \boldsymbol{c}$, $\boldsymbol{d}$, and $\boldsymbol{c}$ directions of the sample parallel to the $\boldsymbol{x}$, $\boldsymbol{y}$, and $\boldsymbol{z}$ axes of the cubes (a procedure for single-crystal orientation described in previous works[58]). These samples allow accurate measurements to be performed as a function of magnetic field orientation in the mutually orthogonal planes ca^*, cb, and a^*b (zx, zy, and xy). All samples were stored below 5 °C to avoid dehydration of the materials during measurements.

B. EPR measurements

EPR spectra of powder and single-crystal samples were collected at Q- and X-bands with ESP-300 ($\nu \sim 33.8$ GHz and ∼9.4 GHz) and EMX Plus (∼9.45 GHz) Bruker spectrometers, using cylindrical cavities with 100 KHz modulation, at room temperature. Powder samples were prepared by finely grinding single crystals, and their composition was verified by x-ray diffraction. Their EPR spectra were measured as a function of T between 10 and 300 K with a Bruker Elexsys E-580 X-band (∼9.47 GHz) spectrometer at the IFSC, Universidade de São Paulo, Brazil. A speck of paramagnetic diphenylpicrylhydrazyl (dpph, $g = 2.0036$) inserted with the sample was used as a field and signal intensity marker. The single-crystal holders were positioned on the horizontal plane on top of a pedestal inside the cavity, and the angular variations of the Q- and X-band spectra were measured as a function of magnetic field orientation $\boldsymbol{h} = (\sin\theta\cos\phi, \sin\theta\sin\phi, \cos\theta)$, where $\boldsymbol{B_0} = B_0\boldsymbol{h}$, in the planes ca^*, cb, and a^*b. In the Q-band measurements, we used a rotating magnet; in the X-band measurements, we rotated the sample holder with a goniometer. The positions of the axes $\boldsymbol{a^*}$, $\boldsymbol{b}$, and $\boldsymbol{c}$ in the a^*b and cb planes were accurately determined considering the C_2 symmetry of the spectra around the $\boldsymbol{b}$ axis. The positions of the $\boldsymbol{c}$ and $\boldsymbol{a^*}$ axes in the ca^* plane were determined by comparison with results in the other planes. This procedure allows an angular accuracy of ∼1° in mounting good-quality single-crystal samples. Positions and widths of the resonances were obtained by least-squares fits of one, two, or three field derivative Lorentzian line shapes to the observed spectra. As usually occurs with Cu^{II} binuclear compounds,[6,57] the samples contain traces (<1%) of mononuclear Cu^{II} ions that show up in their spectra at low T. Due to the higher sensitivity and resolution, Q-band measurements allowed results of higher quality than X-band measurements. However, the X-band results are coherent with those obtained at Q-band, and they provide additional information.

C. Computer programs

The EasySpin package of programs (version 3.1.6),[59] working under Matlab,[59] was used for the EPR spectral simulations and fits along this work. Other calculations were

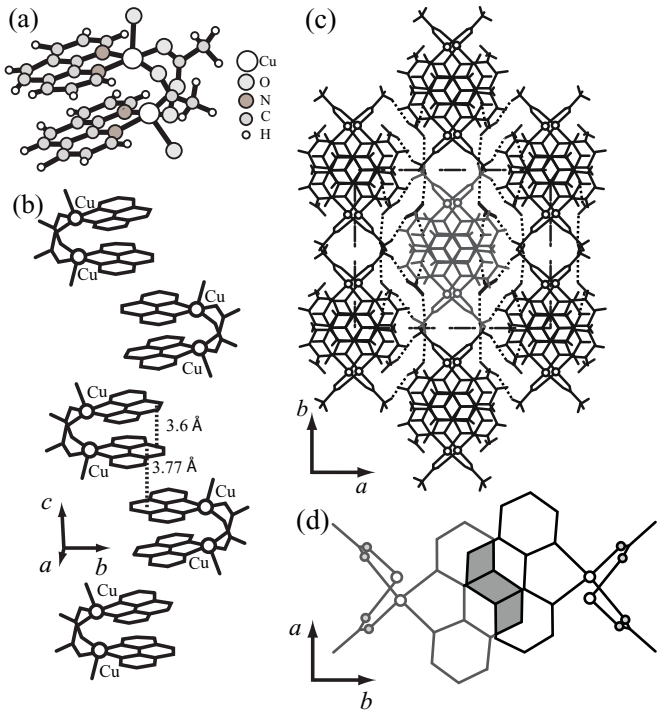

FIG. 1. (Color online) (a) Molecule of $Cu_2ac_2phen_2$ according to Tokii.[57] For simplicity, the NO_3 anions and the water molecules are not included. (b) A chain of binuclear molecules along the z axis. Average distances between the phenanthroline rings are indicated. (c) View of the 3-D array viewed along the direction of the chains. (d) Phenanthroline molecules of neighbor units in a chain showing in gray the stacking region of the rings (33%) at a distance of 3.77 Å.

performed with Matlab. The quality of the spectral simulations was characterized by their rms deviations defined as:

$$\sigma = \sqrt{\frac{1}{N_p}\sum_i \left(S^i_{exp} - S^i_{sim}\right)^2},$$

where S is the signal amplitude (experimental or simulated), and the sum is over the N_p points i of the spectra. The σ value was minimized when fitting models to the experiments.

III. STRUCTURE OF THE COMPOUND AND EXCHANGE PATHWAYS

Figure 1(a) displays the molecular structure of $Cu_2ac_2phen_2$ as determined by Tokii *et al.*.[57] These binuclear units have C_2 symmetry around the $\boldsymbol{b}$ axis, with the two Cu^{II} ions at 3.063 Å along the $\boldsymbol{c}$ axis. The intra-binuclear exchange interaction is mainly supported by two symmetry related O-C-O bridges with C-O distances 1.218 and 1.273 Å and angle 126.1°. The phenanthroline rings of a unit are at an average distance of ∼3.6 Å and angle of 5.2°. Phenanthroline rings of neighbor binuclear units are parallel, the distance is 3.77 Å, and the resulting ring stacking provides exchange paths connecting neighbor binuclear units related by an inversion operation, and gives rise to chains of magnetically identical binuclear molecules along the crystal $\boldsymbol{c}$ axis (see Fig. 1(a)). Figure 1(c) displays a central chain and its six neighbor chains viewed along the $\boldsymbol{c}$ axis, which is also the symmetry axis of the unit. The distance between the axes of nearest neighbor chains is 11.7 Å, and the paths connecting copper atoms in these chains are long and sinuous. Therefore, the exchange couplings between coppers in neighbor chains are negligible. Figure 1(d) sketches the stacking region of the phenanthroline rings of neighbor molecules, which amounts to ∼33% of their total area. We conclude that the spin dynamics in $Cu_2ac_2phen_2$ are essentially along chains parallel to the axial direction of the binuclear units, supported by the stacking of the phenanthroline rings.

IV. EPR SPECTRA

A. Uncoupled binuclear units

Uncoupled AFM binuclear units of spins S_1 and $S_2 = \frac{1}{2}$ are described by the spin Hamiltonian operator of Eq. (2), neglecting the couplings between spins in neighbor units:[4,53]

$$H_0 = -J_0[S(S+1)/2 - 3/4] + (\mathbf{S}.\boldsymbol{D}.\mathbf{S} - \mathbf{s}.\boldsymbol{D}.\mathbf{s}) + \mu_B(\mathbf{S}.\boldsymbol{g_0} + \mathbf{s}.\boldsymbol{G}).\boldsymbol{B_0},$$

where[46,61]

$$\boldsymbol{g_0} = (\boldsymbol{g_1} + \boldsymbol{g_2})/2,\ \boldsymbol{G} = (\boldsymbol{g_1} - \boldsymbol{g_2})/2,\quad \mathbf{S} = \mathbf{S}_1 + \mathbf{S}_2,\quad \mathbf{s} = \mathbf{S}_1 - \mathbf{S}_2 \text{ and } \boldsymbol{D} = \boldsymbol{D_{12}}/2,$$

The total spin is $S = 0$ or $S = 1$ for the singlet and triplet states, respectively, and the term $-\mathbf{s}.\boldsymbol{D}.\mathbf{s}$ has zero matrix elements within the spin triplet responsible of the EPR signal. Since $\boldsymbol{g_1}$ and $\boldsymbol{g_2}$ are related by a C_2 rotation around $\boldsymbol{b}$, $\boldsymbol{G}$ is not zero, and the Zeeman contribution $\mu_B\ \mathbf{s}.\boldsymbol{G}.\boldsymbol{B_0}$ would split each fine structure peak into two components, which is not observed. This term does not commute with the inter-binuclear exchange coupling, and it is randomly modulated and averaged to zero. Thus, the spectra of uncoupled binuclear units are explained with the spin Hamiltonian:

$$H_0 = \mathbf{S}.\boldsymbol{D}.\mathbf{S} + \mu_B\ \mathbf{S}.\boldsymbol{g_0}.\boldsymbol{B_0} \tag{3}$$

with effective spin $S = 1$, where the unimportant constant term was neglected. Considering the C_2 symmetry of the units around the $\boldsymbol{b}$ axis, the xy and zy elements of the $\boldsymbol{g_0}$ and $\boldsymbol{D}$ matrices in Eq. (3) should be zero in the system of axes $\boldsymbol{xyz} \equiv \boldsymbol{a^*bc}$. The binuclear molecules are magnetically identical, and for any orientation of the magnetic field, one observes two allowed transitions, $S_z = \pm 1 \leftrightarrow 0$ and one forbidden transition $S_z = +1 \leftrightarrow -1$.[4,5,8] The four non-zero components of the $\boldsymbol{g_0^2}$ matrix and the three components of the traceless $\boldsymbol{D}$ matrix should be evaluated from the angular variation of the position of the resonances in single crystals or from the powder spectra.[4,5,8,53,59] To simulate powder spectra, one needs to propose, besides the parameters of Eq. (3), an angular variation of the line width, which minimally requires three more parameters. Thus, simplifications of the model are necessary in order to fit spectra of powder samples. EPR data as a function of field orientation in single crystals provide in principle more information because the values of the line width are not needed to fit the angular variation of the line positions. The program EasySpin[59] is appropriate for simulating spectra and fitting a spin-Hamiltonian to the spectra of powder and single crystals. We performed detailed fittings of Eq. (3) to powder and single-crystal spectra, but for simplicity, we

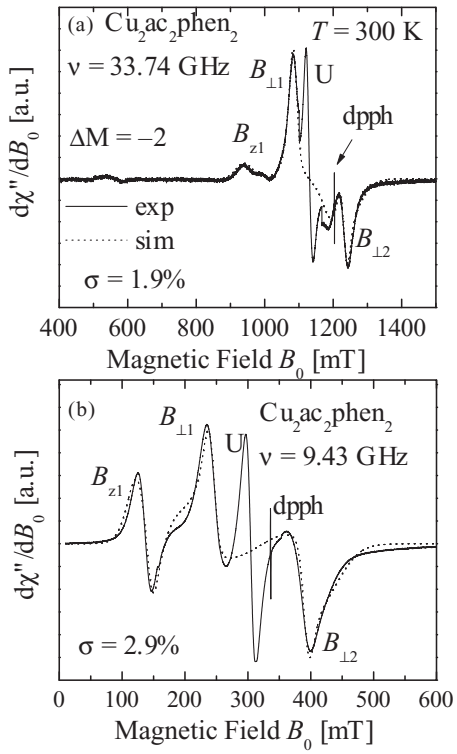

FIG. 2. Powder EPR spectra at room temperature for $Cu_2ac_2phen_2$ at Q-band (a) and X-band (b), normalized to the same peak-to-peak span. Solid and dotted lines are experimental results and simulations obtained as explained in the text. The magnetic field ranges of the U-peaks were not included in the fits of the spectra.

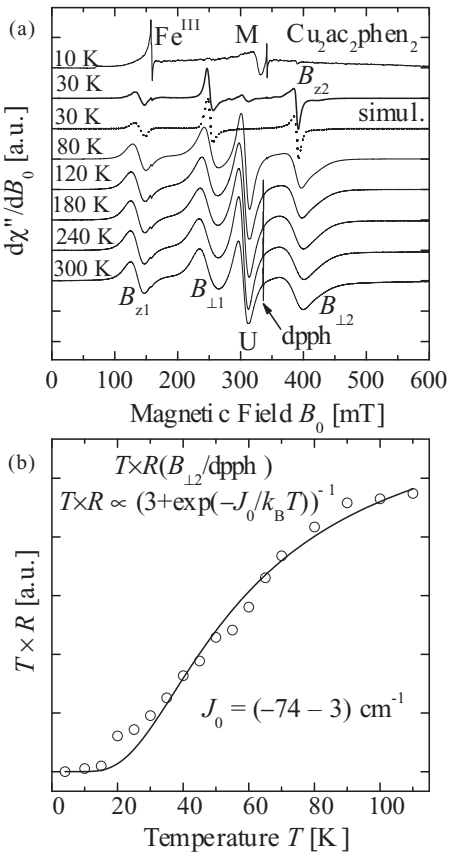

FIG. 3. (a) EPR spectra at X-band of a powder sample of $Cu_2ac_2phen_2$ at selected T between 10 and 300 K. The spectra are normalized to the same peak-to-peak span of the allowed peaks $B_{\perp 1}$ and $B_{\perp 2}$. The small peak at 157 mT arises from Fe^{III} impurities in the sample tubes. The peak M at $g \sim 2.1$, the intensity of which increases with decreasing temperature, is assigned to monomeric Cu^{II} impurities. We emphasize the spectrum at 30 K and include its simulation as a dotted line. At this T, the U-peak is absent. (b) Temperature variation of the ratio R between the integrated areas of the binuclear peak $B_{\perp 2}$ and the dpph marker, multiplied by T. The solid line is the best fit of the Bleaney-Bowers equation to the data.

describe only qualitatively the results of fitting data in powders, except when new information is added, in which case we give the values of the parameters obtained from single-crystal data. In a following section, we analyze the effects of the inter-binuclear couplings using Eq. (2).

B. Powder samples

Figures 2(a) and 2(b) displays the EPR spectra of powder samples obtained at 300 K and Q- and X-bands with the peaks $B_{z1}, B_{\perp 1}$, and $B_{\perp 2}$ labeled according to the standard notation,[7,8,50,51] with the weak peak B_{z2} hidden by the stronger peak $B_{\perp 2}$. The narrow peaks at 1203 mT and 336 mT arise from the dpph marker. The spectra also display an intense and wide unexpected peak at 1130 mT at Q-band and 305 mT at X-band, hereafter called "U"-peak, which is not expected for a binuclear unit and which is too strong to be attributed to contamination with paramagnetic mononuclear spins,[6] the origin of which is discussed later. The weaker forbidden transition $S_z = +1 \leftrightarrow -1$ is at ~556 mT at Q-band, and overlaps the B_{z1} transition at X-band (see Figs. 2(a) and 2(b)).

We fitted Eq. (3) to the powder spectra at 33.74 and 9.43 GHz, and 300 K, excluding the field ranges where the U-peaks appear. We concluded that the parameters have approximate axial symmetry[8] (*i.e.*, $g_{xx} = g_{yy} = g_{\perp}$ $g_{zz} = g_{//}$; $D = 3/2D_{zz}$, $D_{xx} \sim D_{yy}$, or $E = [D_{xx} - D_{yy}]/2$ small), and rotations of the principal axes of the $\boldsymbol{g}$ and $\boldsymbol{D}$ matrices around the $\boldsymbol{b}$ axis are not detected within the uncertainties of the fittings of the powder data. The calculated spectra at 300 K, shown in dotted lines in Figs. 2(a) and 2(b), are in good agreement with the observations, except in the field ranges of the U-peak, which was excluded from the fit. The rms deviations of the simulations calculated excluding these field ranges, as a consequence of the simple model assumed in the angular variation of the widths of the lines, and neglecting the interactions between binuclear units in Eq. (3), are shown in Fig. 2(a) and 2(b).

We also measured the powder spectra at 9.47 GHz in the T range between 4 and 300 K. Spectra at selected temperatures are displayed in Fig. 3(a) normalized to the same amplitude span. The peaks B_{z1}, $B_{\perp 1}$, and $B_{\perp 2}$ in Fig. 3(a) narrow and decrease in intensity for decreasing T. No signals of binuclear units are observed below 20 K, and the weak peak B_{z2} becomes visible at low T (see Fig. 3(a)) when the peak $B_{\perp 2}$ narrows. As an example, we emphasize in Fig. 3(a) the powder spectra of $Cu_2ac_2phen_2$ observed at 30 K, adding the simulations (dotted line with $\sigma = 2.0\%$) that best fit Eq. (3) to this spectrum. The intensity of the U-peak decreases with decreasing T faster

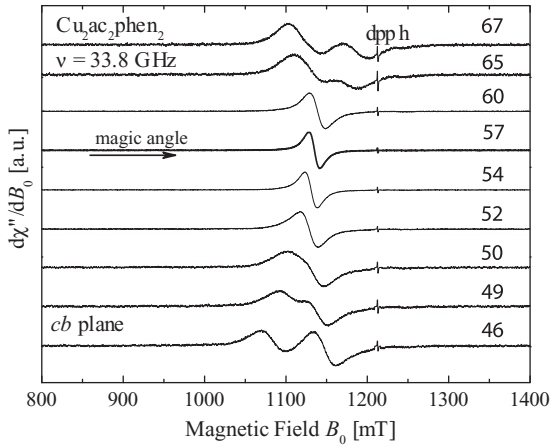

FIG. 4. EPR spectra measured in the *cb* plane in the neighborhood of the magic angle with the peak-to-peak span normalized. Fitting these spectra to Lorentzian line shapes allows us to obtain the position and width of the spectra.

than the standard binuclear peaks, and it disappears when the binuclear transitions are still observed. The agreement between simulated and experimental spectra is much better at low T than at 300 K (compare Figs. 3(a) and 3(b)), which is attributed to the decrease of the U-peaks at low T. From the data in Fig. 3(a), we calculated the ratio $R(T)$ between the integrated area of the peak $B_{\perp 2}$ and that of the dpph marker, as a function of T. Figure 3(b) displays the values of $T \times R(T)$ as a function of T and allows J_0 to be calculated using the Bleaney-Bowers equation,[1,3,6,11,51,54,56]

$$T \times R(T) \propto \frac{1}{3 + \exp(-J_0/k_B T)},$$

where k_B is the Boltzmann constant used to obtain $J_0 = (-74 \pm 3)\ \mathrm{cm}^{-1}$ for the exchange coupling, with statistical coefficient $r = 0.9964$, giving a value smaller than that obtained ($-86\ \mathrm{cm}^{-1}$) from magnetic susceptibility data by Tokii *et al.*[57]

C. Single-crystal samples

Figure 4 displays nine spectra obtained at the Q-band with the magnetic field in the *cb* plane of a single-crystal sample, in a narrow angular range around the "magic angle" at ~57° with the ***c*** axis. They contain one or two peaks depending on field orientation. A third and weaker peak, corresponding to the forbidden transition $S_z = \pm 1 \leftrightarrow \mp 1$, is also observed at ~550 mT ($g \sim 4.2$) for most field orientations, but it is outside of the field range of these figures. Similar spectra were collected in the ca^*cb and a^*b planes at Q- and X-bands, and the positions B_0 and widths Γ_{obs} of these peaks were calculated by fitting Lorentzian derivative line shapes to the experimental spectra. We used these values to construct the angular variation of the positions (Figs. 5 and 6) and widths (Fig. 7) of the resonances at both microwave frequencies.

Figures 5(a) and 6(a) show the spectra at Q- and X-bands for the applied field along the ***c*** axis; they display two main peaks corresponding to the allowed transitions, in agreement with the predictions of Eq. (3). The results for the positions at Q- and X-bands as a function of the orientation of B_0 in the three studied crystal planes are displayed in Figs. 5(b)–5(d)

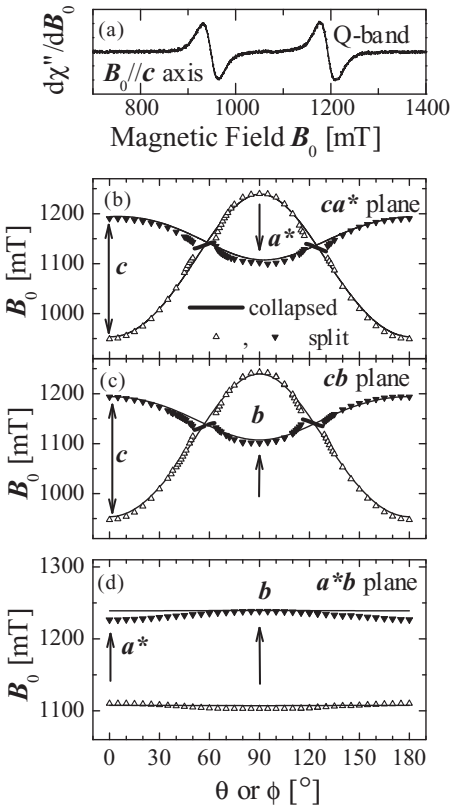

FIG. 5. (a) EPR spectrum observed for the magnetic field along the ***c*** axis at $\nu = 34.0$ GHz. (b–d) Angular variation of the positions of the two allowed resonances $\pm 1 \leftrightarrow 0$ observed with B_0 in the three crystal planes. Symbols are experimental values. The lines are obtained from the fit of (3) to the data. The global rms deviation between fitted and experimental values in the three planes is $\sigma = 0.3\%$.

and 6(b)–6(d), respectively. As expected from the crystal symmetry, the angular variations of the positions of the resonances in the planes a^*b and cb are symmetric around the ***b*** axis. The single-crystal data at X-band are qualitatively similar to that at Q-band but have a larger dispersion. The spectra observed in single crystals at both microwave frequencies and for any orientations of B_0 do not contain an unexpected signal in the field region where the U-peak appears in the powder spectra (compare Fig. 2(a) and 2(b) with 5(a) and 6(a)).

In most of the angular ranges of Figs. 5(b) and 5(c) and 6(b) and 6(c), the positions of the peaks of the spectra in the ca^* and cb planes display a "dipolar-type" angular variation described by $f(\theta) \propto \pm\frac{1}{2}(3\cos^2\theta - 1)$ around a central field position, where $\theta = 0$ corresponds to the axial direction of the binuclear units. However, and as shown in Figs. 4, 5(b) and 5(c), and 6(b) and 6(c), instead of observing simple crossings at the "magic angles" where $f(\theta) = 0$, we observe that the two lines suddenly merge and stay merged in an angular range around this angle. In these angular ranges, one observes a single peak at the barycenter of the positions where the two fine structure peaks would be expected, as observed previously for other binuclear compounds.[53]

The peak-to-peak widths of the lines at Q- and X-bands in the three studied planes displayed in Figs. 7(a)–7(f) are relatively constant, except around the magic angles (planes ca^* and cb), where the fine structure peaks collapse to a

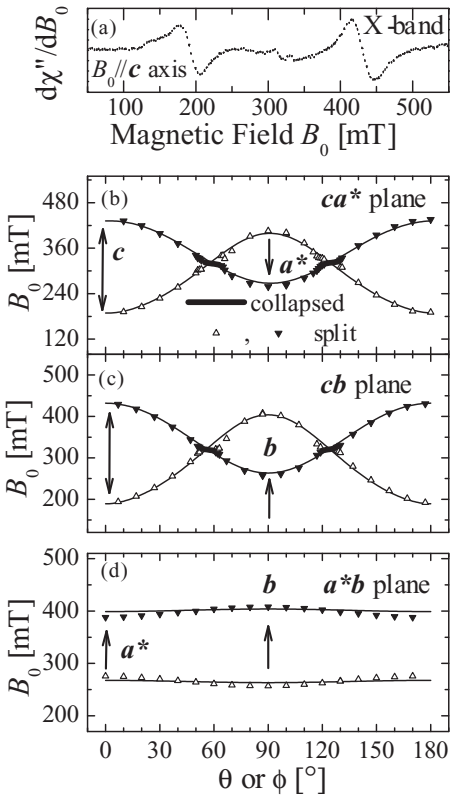

FIG. 6. (a) EPR spectrum observed for the magnetic field along the $\boldsymbol{c}$ axis at $\nu = 9.45$ GHz. (b–d) Angular variation of the positions of the two allowed resonances $\pm 1 \leftrightarrow 0$ observed with B_0 in the three crystal planes. Symbols are experimental values. The solid lines are obtained using the parameters obtained from the fit of Eq. (3) to the Q-band data. The global rms deviation between calculated and experimental values of the line position in the three planes is $\sigma = 2\%$.

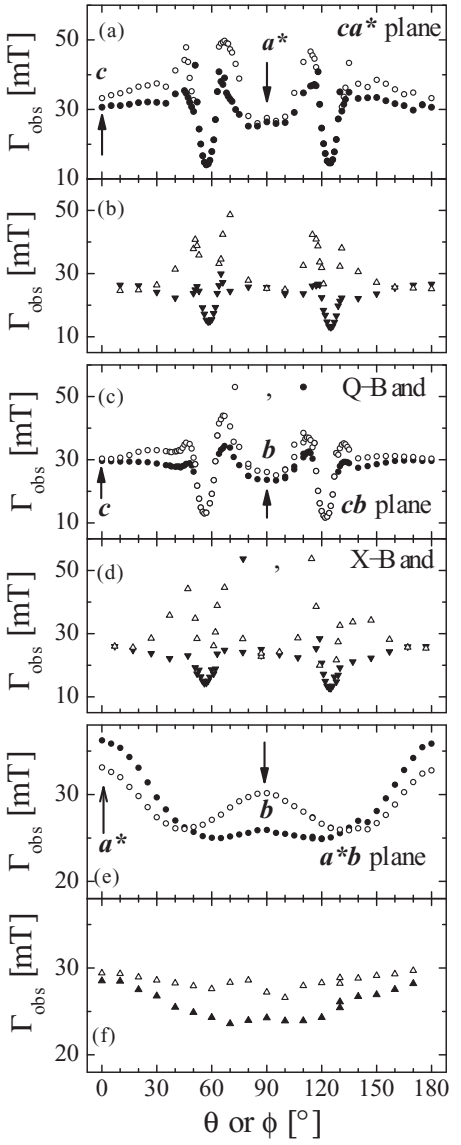

FIG. 7. Width Γ_{obs} of the lines observed at Q- and X-bands in the three crystal planes, $\boldsymbol{ca^*}$, $\boldsymbol{cb}$, and $\boldsymbol{a^*b}$ of a single-crystal sample.

single resonance, and a significant narrowing with a parabolic dependence is observed. The narrowing that occurs when approaching to the magic angle is also observed in Fig. 4.

We obtained the parameters of Eq. (3) by fitting this Hamiltonian to the angular variations of the positions of the resonances observed at each microwave frequency in the three planes, in the angular ranges where they are not collapsed. Two principal values of the $\boldsymbol{g_0}$ matrix are equal within the accuracy of the fitting. Also, one principal value of the $\boldsymbol{g_0}$ and $\boldsymbol{D}$ matrices is along the $\boldsymbol{z}$ axis, and rotating these matrices around the $\boldsymbol{b}$ axis (which is allowed according the point symmetry of the binuclear units), angles smaller than 1° do not change significantly the quality of the fit. So, we neglected these possible rotations and obtained from the Q-band data the principal values $g_\perp = 2.070 \pm 0.005$ in the xy (a^*b) plane and $g_{//} = 2.269 \pm 0.005$ along the $\boldsymbol{z}$ ($\boldsymbol{c}$) axis. The fine structure tensor $\boldsymbol{D}$ has a principal value $D = -3850 \pm 50$ MHz along the $\boldsymbol{z}$ axis and $E = -53 \pm 30$ MHz in the perpendicular plane. In this calculation, we consider only the angular regions far from the magic angles, where the fine structure peaks are split. The sign of D, not verified in our experiments, is taken from experimental and theoretical results in tetracarboxylate "paddlewheel" binuclear units.[20,62] The calculated angular variations of the positions of the peaks, included as solid lines in Fig. 5(b)–5(d), are in good agreement with the data ($\sigma = 0.3\%$), except in the angular regions where the peaks collapse. The fitting of the single-crystal results at X-band (Figs. 6(b)–6(d)) is poorer than that at Q-band, but it is in good agreement within uncertainties. Since the parameters obtained at Q-band reproduce well the experimental values at X-band (rms deviation $\sigma = 2\%$), see solid lines in Figs. 6(b)–6(d), we use these values in all calculations.

Figures 8(a)–8(d) displays the ratio K between the experimental and calculated fine structure splittings as a function of the inverse of the calculated splitting, describing with greater detail the collapse of the resonances around the magic angles. Figure 9(a)–9(d) displays the width Γ_{obs} of the merged line as a function of magnetic field orientation at Q-band. We analyze the results in these figures in terms of the inter-binuclear interactions. The variation of the width in the a^*b plane does not show special features.

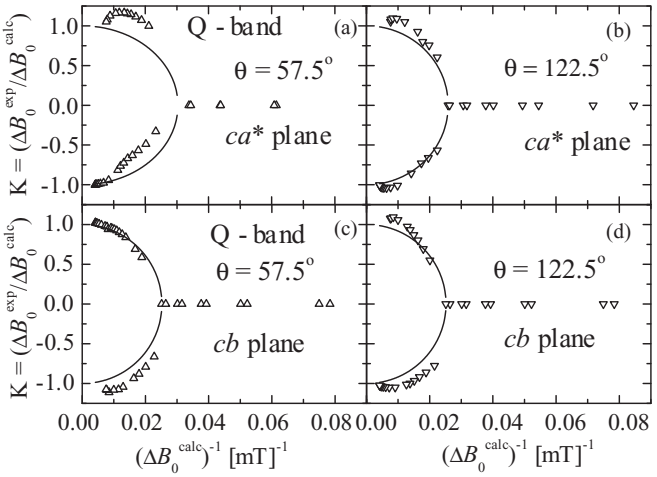

FIG. 8. Ratio K between the observed $\Delta B_0^{\exp}$ and calculated ΔB_0^{calc} splittings of the fine structure peaks for a single crystal of $Cu_2ac_2phen_2$ as a function of $(\Delta B_0^{\text{calc}})^{-1}$, as observed in the neighborhood of the magic angles at Q-band (Figs. 5(b)–5(c)). Symbols are experimental values, and solid lines are fittings of (6) to the data. Graphs (a), (b), (c), and (d) refer to the two magic angles, in the ca^* and cb planes.

D. The central U-peak of the powder spectra

A U-peak in the powder spectra of binuclear compounds was observed but not explained by several previous authors.[63] In a recent investigation of a chain of coupled binuclear units,[54] we observed a U-peak and attributed it to the collapse of the resonances around the magic angles due to the interactions between the binuclear units, but we had no single-crystal data to prove our hypothesis. Now the single-crystal measurements (Figs. 5 and 6) provide full proof of the origin of this U-peak. The powder spectra at Q- and X-bands and 300 K are plotted in Fig. 10(a) and 10(b). Figure 10(c) and 10(d) displays the observed angular variation of the positions of the resonances at the same frequencies and T, including the collapsed peaks close to the magic angles, using the same field scale. This presentation of the experimental results explains the known sources of the peaks B_{z1}, $B_{\perp 1}$, $B_{\perp 2}$, and B_{z2} as turning points of the angular variations, where the signal accumulates in the spectrum of a randomly distributed collection of crystallites.[8] It also shows that the observed collapse of the fine structure around the magic angles (see Figs. 5(b)–5(c), 6(b)–6(c), and 8(a)–8(d)) and the simultaneous narrowing of the collapsed line (see Figs. 7(a)–7(d) and 9(a)–9(d)) in the single-crystal spectra are the source of the U-peak of the powder spectrum. Since we measured both, the collapse of the single-crystal peaks and its effect in powder samples, we verify our hypothesis. The quality of the fittings of the powder spectra is better at low temperature, when the U-peak disappears, indicating that its growth at higher T produces a deformation of the spectrum from that expected for an uncoupled unit. It is worthwhile to note that the intensity of the U-peak and its temperature variation clearly reflect the origin of the peak proposed here. This intensity increases with increasing T when the angular range of the collapsed region widens because the population of the triplet state increases, and the mean inter-binuclear interaction grows.

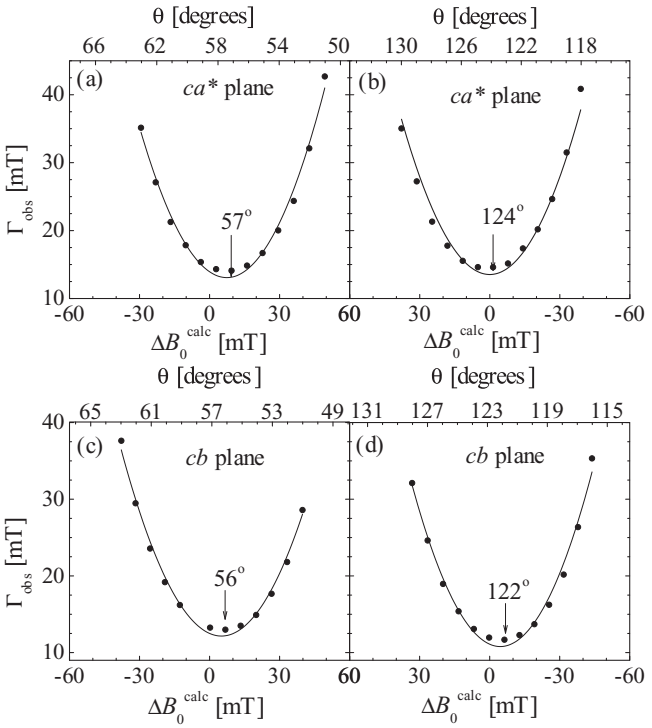

FIG. 9. Peak-to-peak line widths Γ_{obs} of the collapsed signals at Q-band (see, Fig. 7(a)–7(d)) in the neighborhood of the magic angles in the ca^* and cb planes, as a function of the distance between peaks ΔB_0^{calc} calculated from the fit of the data. Graphs (a), (b), (c), and (d) refer to the two magic angles, in the ca^* and cb planes. The solid lines were obtained from fits of Eq. (7) to the data.

V. DISCUSSION

The most relevant features of the EPR results are:

(i) the merging of the fine structure peaks observed around the so-called "magic angles," displayed in Figs. 5, 6, and 8 as observed at Q- and X-bands;

(ii) the narrowing of these peaks, coincident with the collapse of the fine structure signal, displayed in Figs. 7(a)–7(d) and 9(a)–9(d); and

(iii) The U-peak of the powder spectra, and their temperature dependence (Figs. 2(a) and 2(b), 3(a), and 10(a)–10(d).

These sources of data provide complementary information about the inter-binuclear couplings and the behavior, localization, and dimensionality of the collective wave functions. Here, we analyze these results using the Anderson-Kubo theory of magnetic resonance,[39,40] which allows the interaction parameters from the experimental data to be evaluated. We also describe qualitatively our EPR results modeling a chain of weakly interacting binuclear units in terms of triplet excitons or triplons,[16,20] and compare the results of the two methods.

A. Anderson-Kubo's theory of exchange narrowing and collapse

Anderson's theory[39] predicts the EPR line shape $I(\omega)$ as:

$$I(\omega) = \frac{1}{2\pi}\int_{-\infty}^{\infty} G(t)e^{-i\omega t}dt,$$

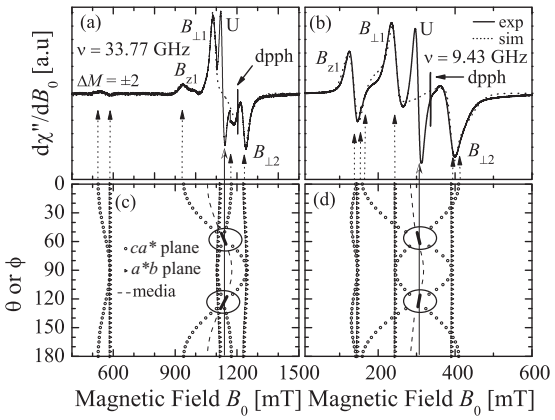

FIG. 10. Origin of the central U-peak in the powder spectra at Q-band (a and c) and X-band (b and d). Dotted lines in (c) and (d) display the angular variations of the positions of the peaks of the single-crystal spectra. The dashed lines are the average positions in the ca^* and cb planes. The peaks of the powder spectra (a and b) arise from the extremes of the angular variation. The collapse of the lines around the magic angles (see ovals in c and d) produces an accumulation of signal in a narrow field range, giving rise to the central peak of the powder spectra.

where

$$G(t) = \int_{-\infty}^{\infty} I(\omega) e^{-i\omega t} d\omega = \frac{\langle M_x(t) M_x(0)\rangle}{\langle M_x(0) M_x(0)\rangle} = \frac{tr\left(e^{-\frac{H}{k_B T}} M_x(t) M_x(0)\right)}{tr\left(e^{-\frac{H}{k_B T}} M_x^2(0)\right)} \quad (4)$$

is the response function of the time-dependent magnetization $M_x(t)$ in the Heisenberg representation:

$$M_x(t) = e^{\frac{iHt}{\hbar}} M_x e^{-\frac{iHt}{\hbar}}.$$

In Eq. (4), the angular brackets indicate thermal averages at temperature T, and tr is the trace of matrix within parentheses. We are interested in the contribution to the time dependence of $M_x(t)$ arising from the stochastic interactions of the binuclear units with the environment, and Kubo describes it as:[41]

$$\frac{dM_x(t)}{dt} = i\,\Omega(t)\,M_x(t),$$

where in our case $\Omega(t)$ is the exchange modulated frequency associated with the anisotropic exchange or dipolar coupling (fine structure) within a binuclear unit shifted to give a mean value $\langle\Omega(t)\rangle = 0$. The random function $\Omega(t)$ is characterized by its second moment Δ, and an *exchange correlation time* τ_{ex}, or equivalently, an *exchange frequency* ω_{ex}, defined by:

$$\Delta = \langle\Omega^2\rangle^{1/2} \text{ and } \tau_{ex} = \frac{2\pi}{\omega_{ex}} = \int_0^{\infty} \frac{\langle\Omega(t)\Omega(0)\rangle}{\Delta^2} dt, \quad (5)$$

which is associated with the inter-binuclear exchange interactions. When the product $\Delta\tau_{ex} > 1$, the stochastic modulation of Ω is slow; if $\Delta\tau_{ex} \ll 1$, the modulation is fast, and the spectrum displays exchange narrowing phenomena. In our experiments, we move between these two conditions and observe the transition that is associated with a change of the wave function of the system from localized in one unit to distributed along the chains. Anderson-Kubo's model was applied to paramagnetic materials with no excited levels, and equal state populations by Passeggi and Calvo,[64] who calculated the relation between ω_{ex} and the exchange couplings J'. The thermal averages in Eq. (5) were made in the high-temperature approximation, *i.e.,* where the density matrix $\exp(-H/k_BT)/\text{tr}[\exp(-H/k_BT)] \sim \mathbf{I}/\text{tr}[\mathbf{I}]$, the normalized unit matrix. This is not normally valid for binuclear systems, where the populations of the low-energy states vary with T. Calculations of temperature-dependent ω_{ex} exist,[65] but not for coupled binuclear systems. Thus, we evaluate ω_{ex} from the data as a phenomenological temperature-dependent parameter related to the inter-binuclear couplings and to T, and later relate these values to the more fundamental interactions J'. Our hypothesis is that at high T, the relations between ω_{ex} and J' obtained by Passeggi and Calvo[64] are valid, but when T decreases, ω_{ex} varies proportionally to the thermal population of the triplet state.

The symbols in Fig. 9(a)–9(d) display the ratio $K = \Delta B_0^{exp}/\Delta B_0^{calc}$ between the observed splitting of the collapsing resonances and that calculated in the absence of interaction, as a function of the reciprocal of the calculated splitting, for the magnetic field oriented near the magic angles in the planes ca^* and cb. This graph, used by Martino *et al.*[44] (see also Refs. 46 and 66) to study the collapse of EPR signals arising from mononuclear species in rotated lattice sites, offers a normalized view of the collapse of the signals and allows the exchange frequency ω_{ex} to be determined. When $(\Delta B_0^{calc})^{-1}$ is large, close to the magic angles, the signals are collapsed, and $K = 0$. When $(\Delta B_0^{calc})^{-1}$ is small, far from the magic angles, $K \sim \pm 1$. The collapse is abrupt and occurs when $g\,\mu_B[\Delta B_0^{calc}]_{collapse} = \hbar\omega_{ex}$, a condition allowing the exchange frequency ω_{ex} to be obtained. Values of ω_{ex} were obtained by fitting the function

$$K = \frac{\Delta B_0^{exp}}{\Delta B_0^{calc}} = \pm\sqrt{1 - \left(\frac{\hbar\omega_{ex}}{g\mu_B \Delta B_0^{calc}}\right)^2} \quad (6)$$

to the data in Fig. 8(a)–8(d) in the noncollapsed region. From the fits of Eq. (6) to the data in Fig. 8(a)–8(d), we obtained values of ω_{ex} with an average

$$\hbar\omega_{ex}(\text{collapse}) = (0.04 \pm 0.01)\ \text{cm}^{-1},$$

and the solid lines in these figures are obtained from this result.

For the angular variation of the observed line width, Γ_{obs}, of the transitions $S_z = \pm 1 \leftrightarrow 0$ in the collapsed regions around the magic angles, Anderson's theory[39] predicts:

$$\Gamma_{obs} = \frac{g\mu_B \left(\Delta B_0^{calc}\right)^2}{\hbar\omega_{ex}} + \Gamma_0, \quad (7)$$

where ΔB_0^{calc} in Eq. (7) is the splitting of the collapsing resonances calculated in the absence of exchange interactions, which can be extracted from the solid lines plotted in Fig. 5(b) and 5(d). Γ_0 is a residual contribution to the line width arising from other broadening sources, considered here as a constant. The average value of ω_{ex} resulting from the fits of (7) to the results in Fig. 9(a)–9(d) is:

$$\hbar\omega_{ex}(\text{narrowing}) = (0.07 \pm 0.01)\ \text{cm}^{-1}.$$

An average of the values of exchange frequency is $\hbar\omega_{ex} = (0.055 \pm 0.015)$ cm^{-1} at room temperature. Considering that this result was obtained in the high-T range ($k_BT \gg J_0$), we use the relationship $2|J'|^2 \approx \hbar^2{\omega_{ex}}^2$ to obtain $|J'| = (0.04 \pm 0.01)$ cm^{-1} between neighboring binuclear units.[53,64] The discrepancies between the values of $\hbar\omega_{ex}$ obtained from the collapse and the narrowing of the peaks of the spectra give an idea of the approximations of the model used in this simple evaluation.

B. Triplet excitons and EPR spectra of a chain of binuclear units

Triplet excitons or triplons can be used to describe the spin dynamics and their effect on the EPR spectra introduced by J'. We introduce here a procedure treating the problem and describing the observed spectral behavior. Considering the chain structure of $Cu_2ac_2phen_2$ and following Lynden-Bell and McConnell (L&M),[16,17] we replace it by an alternating chain of spins $\frac{1}{2}$ described by:

$$H_{ch} = -\sum_{n} [J_0 \mathbf{S_{2n}}.\mathbf{S_{2n+1}} + J' \mathbf{S_{2n}}.\mathbf{S_{2n+1}}] + H_{fs}, \qquad (8)$$

where $\mathbf{S_i}$ is the operator of the ith spin $\frac{1}{2}$ in the chain. We added to the results of L&M the term H_{fs}, summed over all binuclear units of the fine structure and Zeeman contributions of individual units defined in Eq. (3). For $J' = 0$, the solutions are the singlet and triplet states with energies $3J_0/4$ and $-J_0/4$, respectively, and the resulting EPR spectrum of the triplet was described before. In the cases of interest, where the excited triplet is thermally accessible, we define operators t_n^+ and t_n, creating or destroying an excitation on unit n (each site may hold only one excitation), to obtain from Eq. (8):[16]

$$H_{ch} = H_{ch}^{(0)} + H_{ch}^{(1)} + H_{ch}^{(2)} + H_{ch}^{(3)} + H_{fs}, \qquad (9)$$

where

$$H_{ch}^{(0)} = -\sum_{n} J_0 t_n^+ t_n;\ H_{ch}^{(1)} = \frac{J'}{4}\sum_{n} t_n^+(t_{n+1} + t_{n-1});\ H_{ch}^{(2)} = -\frac{J'}{4}\sum_{n} \mathbf{S_n}.\mathbf{S_{n+1}}; \qquad (10)$$

and $H_{ch}^{(0)}$ is the energy arising from the excited triplets. We propose that $H_{ch}^{(0)} + H_{fs}$ gives rise to the EPR spectrum of the uncoupled chain of units that, in the presence of J', is distorted and changed by the other contributions to H_{ch}. The hopping term $H_{ch}^{(1)}$ contains interactions between adjacent excited units that transfer excitations from one site in the triplet state to a neighbor site in the singlet state, contributing to spin delocalization. The operators $\mathbf{S_n}$ act on the total spin of the binuclear units, and $H_{ch}^{(2)}$ includes terms like $S_n^+ S_{n+1}^-$, which produce spin flips in neighbor units in the triplet state, leaving unchanged the triplet population. $H_{ch}^{(3)}$ (not shown) has matrix elements between states with different numbers of excitations.

A basis state of a chain of N_S spins with p excitations located in sites $n_1, n_2, \ldots, n_p$ is written as:

$$\Psi_\alpha = \sum_{n_1 \langle n_2 \langle \ldots \langle n_p} C_\alpha(n_1, n_2, \ldots, n_p)|n_1\sigma_1, n_2\sigma_2, \ldots, n_p\sigma_p\rangle,$$

where σ_i represents the spin component ($\sigma_{zi} = 1, 0, -1$) of the triplet state at site n_i. For $k_BT < J_0$, when the number of excitations is low, few state vectors with triplet excitations at neighbor sites occur, and they can be ignored. Thus, Eqs. (9) and (10) are simple to treat because $H_{ch}^{(2)}$ and $H_{ch}^{(3)}$ do not contribute, a case solved by L&M[16] with some detail. The eigenvalues and secular equations of $H_{ch}^{(0)} + H_{ch}^{(1)}$ are:

$$\left(H_0 + H_{ch}^{(1)}\right)\Psi = E\ \Psi,$$

$$(pJ_0 - E)\ C(n_1, n_2, \ldots, n_i, n_p) + \frac{J'}{4}\sum_i [C(n_1, n_2, \ldots, n_i + 1, \ldots n_p) - C(n_1, n_2, \ldots, n_i - 1, \ldots n_p)] = 0,$$

with the solution:

$$C(n_1, n_2, \ldots, n_p) = \sum_{\lambda=1}^{p!} a_\lambda P_\lambda\ \exp\left(i\sum_\nu k_\nu n_\nu\right),$$

where P_λ and a_λ are an operator producing one of the p! permutations of the p numbers ($n_1, n_2, \ldots, n_p$) and an arbitrary coefficient for the state, and the wave vectors $k_\nu = 2\pi\ m_\nu/N$ ($m_\nu = 0, 1, 2, \ldots$) are the momenta of the excitons having energies:

$$E = -pJ_0 + \sum_{\nu=1}^{p}\frac{J'}{2}\cos(k_\nu).$$

There is also a wave vector dependence of the fine structure term H_{fs} that can be written for the case of axial symmetry as:[16]

$$D_\nu = D + D'\ \cos(k_\nu), \qquad (11)$$

where D is the fine structure parameter for uncoupled units, and D' is proportional to J'. The EPR spectra of interacting units cannot distinguish the wave vector dependence of the fine structure parameter of Eq. (11), which contributes only as a uniform line width of the fine structure peaks.

The hopping of the excitations produced by $H_{ch}^{(1)}$ delocalizes the triplets in the chain and destroys the hyperfine structure,[17,67] because more copper nuclei are involved in the coupling. This could happen at relatively low T, when $H_{ch}^{(1)}$ is already operative. This has been observed by many authors, and was discussed by Soos.[17,67] However, $H_{ch}^{(1)}$ does not change the fine structure (except the aforementioned uniform broadening), because the fine structure is equal for all binuclear units in the chains of $Cu_2ac_2phen_2$. To explain the observed collapse, we have to consider the contribution $H_{ch}^{(2)}$ acting on neighbor triplet sates in the chain, and changing their relative spin orientation. To occur, this needs a higher T in order to have a higher population of the triplet state. The terms type $S_n^+ S_{n+1}^-$ (n labels the binuclear unit in the chain) produce stochastic spin flips of the values of S_{nz} of neighbor units with frequency ω_{ex}, proportional to J', thus averaging to zero the zero field splitting when $\hbar\omega_{ex}$ becomes larger than the zero field splitting. In fact, it destroys not only the fine structure, but also the broadening produced by the wave vector dependence of the fine structure Eq. (11), thus narrowing the line. These effects, which are

observed in our single-crystal EPR experiments, are discussed below.

As explained previously, the value of ω_{ex} has a T dependence arising from the change of the population of the triplet states in the chains. This T dependence could in principle be evaluated by performing detailed single-crystal experiments such as those described in Figs. 5 and 6. These experiments are difficult to perform, but the collapse of the fine structure can also be observed in the U-peak of the powder spectra for which amplitude is proportional to the number of units with collapsed fine structure.

Our model for the collapse of the fine structure is also supported by the behavior of the line width in the angular ranges where the collapse occurs (Figs. 7(a)–7(d) and 9(a)–9(d)). The narrowing observed is due to the destruction of the contribution to the broadening produced by the wave vector dependence of the fine structure parameter Eq. (11). This contribution is averaged out, and consequently a narrowing of the line occurs superimposed on the collapse of the fine structure. The parabolic shape of the narrowing around the center of the collapse (Fig. 9) is a consequence of the effectiveness of the collapse, which is largest at the magic angles. More detailed calculations are needed to apply elementary excitations to predict EPR spectra in coupled spin systems, and we are working in this direction. However, the model described here is capable of describing the experimental results.

C. Comparison with EPR results in related systems

Exchange interactions coupling polynuclear units interested chemists and physicists along the years because of their importance in molecular magnets,[4,6] and in the various applications of the theories of many spin systems to important physical problems. It is clear that susceptibility measurements are not appropriate to evaluate these couplings because their contributions are much smaller than others, and molecular field calculations or measurements at lower T cannot separate them. EPR seems to be an appropriate technique for the purpose, and Soos[67] and Valentine *et al.*[52] reported early studies of the effects of inter-binuclear interactions in the fine and hyperfine structure of the EPR spectra considering the role of elementary excitations. Their work is closely related to that of Lynden-Bell and McConnell[16] and of Nordio,[17] discussed before. More recently, Zvyagin *et al.*,[35,68] reported X-band EPR spectra of single crystals of the binuclear compound $BaCuSi_2O_6$, a material having copper binuclear units with $J_0 = -35$ cm^{-1} and $J' = -1.5$ cm^{-1} that shows field-induced Bose-Einstein condensation of triplons.[32,33] At room temperature, they observed a single EPR peak (no fine or hyperfine structure), the angular variation of which is determined by the g-factor. When the temperature decreases below ~10 K, the single peak broadens and then splits in two peaks corresponding to the expected fine structure. At lower T (~6 K), the spectrum also displays a four-line hyperfine group corresponding to mononuclear Cu^{II} defects present in the sample. They also report the angular variation of the spectrum observed at 6 K in a plane containing the axis of the binuclear unit showing the angle dependence described above for a binuclear unit. However, no sudden transition of the fine structure peaks close to the magic angles was observed, maybe because they occur in narrow angular ranges, or because this possibility was not considered in the analysis of the data. The model introduced by us to explain our data in $Cu_2ac_2phen_2$ clearly describes the results in $BaCuSi_2O_6$, even if in that case J_0 is smaller and J' much larger than for our compound. The main differences are in the temperature scales that are determined by the values of J_0 and J'. In their experiments, they vary ω_{ex}, changing the temperature of the sample and, consequently, the population of the triplet state. The fine structure merges and collapses at higher T, when the triplet state population is high, and triplet-triplet interactions are more effective. Meanwhile, the destruction of the hyperfine structure of *mononuclear* Cu^{II} ions occurs at lower T, when the hopping processes are important; and the hyperfine structure of the *binuclear* Cu^{II} units may have merged and collapsed at temperatures lower than those studied. In fact, the hyperfine splitting of dinuclear units is half of the mononuclear copper, and the collapse of that structure would occur at lower T than for mononuclear spins, when the inter-binuclear coupling and, consequently, the value of ω_{ex} are smaller. The explanation of the destruction of the fine structure in terms of triplet excitations introduced by Zvyagin *et al.*. is different than ours.[35,68] They attribute it to the hopping of the triplet excitations, and propose that in the high-T range where most of the binuclear units are in the triplet state, fine structure destruction is not effective because hopping processes are impeded. In our explanation, hopping is not important to destroy the fine structure, which is mostly affected by spin-flip processes between neighbor triplet states that occur at higher T.

Sebastian *et al.*[33,34] performed EPR studies of $BaCuSi_2O_6$ in a range of microwave frequencies between 26 and 660 GHz. Their data at 51.8 GHz, which are described in detail, are very similar to those of Zvyagin *et al.*,[35] with differences expected by the higher microwave frequency. Camara *et al.*[11] reported X-band EPR measurements in three binuclear compounds of V^{IV} ions ($S = 1/2$). Their EPR results are also compatible with the above-mentioned authors.

In our opinion, the advantage of binuclear compounds like $Cu_2ac_2phen_2$, with a higher value of J_0 and much smaller value of J', is that they allow greater detail to be observed in the evolution of the EPR spectra with the changes of the exchange frequencies with temperature and of the energy levels with magnetic field orientation, providing a clearer view of the effects of the spin dynamics produced by J'. Our results allow clear transitions to be distinguished between quantum dynamical regimes, thus providing more information and greater possibilities of modeling.

VI. CONCLUSIONS

Using EPR, we studied the compound $Cu_2ac_2phen_2$ displaying a 1-D array of weakly coupled AFM binuclear units. Measurements in powder and single-crystal samples between 10 and 300 K allow $J_0 = (-74 \pm 3)$ cm^{-1} and $|J'| = (0.04 \pm 0.01)$ cm^{-1} ($|J'/J_0| = 5.4\times10^{-4}$) to be obtained for the intra- and inter-binuclear couplings. J' is supported by the stacking of the phenanthroline rings of neighbor units, and the main results are listed at the beginning of the previous chapter.

We explain the changes in the fine structure components of the excited triplet state using the classical theory of

Anderson and Kubo[38–41] of exchange narrowing and collapse. Considering the exchange couplings between neighbor units (Fig. 1(b), the sharp collapse of the resonances is interpreted as a dimensional quantum phase transition between a zero-dimensional binuclear unit and a 1-D spin chain. In this image, the exchange narrowing phenomenon is a *discontinuous* transition occurring when the average stochastic distribution of local exchange fields acting on a binuclear unit equals the fine structure splitting of the spin triplet (D-term arising from intra-binuclear dipole-dipole and anisotropic exchange).

We also analyze the data in terms of elementary excitations or triplons arising from the inter-binuclear couplings to conclude that the interaction between triplons is responsible of the observed collapse of the fine structure. The hopping of the excitations may destroy the hyperfine structure, but it is not effective with the fine structure of the spectra, where spin-flip transitions of neighbor triplets are responsible for the fine structure collapse. Our model also explains the large narrowing of the peaks of the spectra produced simultaneously with the collapse of the fine structure. This explanation is different from that given by Zvyagin *et al*.[35] to explain similar data for other binuclear compounds.

The intra-binuclear coupling $|J'| = (0.04 \pm 0.01)$ cm^{-1} evaluated here is supported by the stacking of the aromatic rings of phenanthroline (see Fig. 1(b) and 1(d)). These noncovalent interactions seem to be important in supramolecular chemistry and in biochemistry,[69] but controversies still exist about the subject.[70] The role of π-π stacking to support exchange couplings has previously been studied by Brondino *et al*.[71] and Neuman *et al*.[55] The values obtained should allow the strength of the exchange interaction to be characterized, giving a tool for a better understanding of the magnitude of the electrostatic coupling. For this purpose, it is important to study compounds where π-π stacking does not compete with other weak couplings. This is the case in $Cu_2ac_2phen_2$ (see Fig. 1(b) and 1(d)), where, in addition, the large value of $|J_0|$ allows clearer experimental procedures to evaluate $|J'|$. More work on the subject is needed to make further progresses.

ACKNOWLEDGMENTS

We are grateful to O. R. Nascimento for allowing us to perform EPR measurements in the range 10–100 K and to M. Perec for helpful comments on the manuscript. This work was supported by a CAI+D-UNL grant in Argentina and by CNPQ in Brazil. R.C. is a member of CONICET, Argentina.

*calvo.rafael@conicet.gov.ar

[1] B. Bleaney, and K. D. Bowers, Proc. R. Soc. London A **214**, 451 (1952).
[2] B. C. Guha, Proc. R. Soc. London A **206**, 353 (1951).
[3] O. Kahn, Angew. Chem. Int. Ed. **24**, 834 (1985).
[4] A. Bencini and D. Gatteschi, *Electron Paramagnetic Resonance of Exchange Coupled Systems* (Springer-Verlag, Berlin, 1990).
[5] J. R. Pilbrow, *Transition Ion Electron Paramagnetic Resonance* (Clarendon Press, Oxford, 1990).
[6] O. Kahn, *Molecular Magnetism* (VCH, New York, 1993).
[7] N. M. Atherton, *Principles of Electron Spin Resonance* (Ellis Horwood: PTR Prentice Hall, New York, 1993).
[8] J. A. Weil and J. R. Bolton, *Electron Paramagnetic Resonance: Elementary Theory and Practical Applications* (Wiley-Interscience, New York, 2007).
[9] T. Giamarchi, C. Rüegg and O. Tchernyshyov, Nature Physics **4**, 198 (2008).
[10] W. H. Armstrong, and S. J. Lippard, J. Am. Chem. Soc. **105**, 4837 (1983); R. Baggio, R. Calvo, M. T. Garland, O. Peña, M. Perec, and A. Rizzi, Inorg. Chem. **44**, 8979 (2005); B. Barja, R. Baggio, R. Calvo, M. T. Garland, M. Perec, and A. Rizzi, Inorg. Chim. Acta, **359**, 3921 (2006).
[11] I. S. Camara, R. Gautier, E. Le Fur, J.-C. Trombe, J. Galy, A. M. Ghorayeb, and A. Stepanov, Phys. Rev. B **81**, 184433 (2010).
[12] R. Calvo, R. E. Rapp, E. Chagas, R. P. Sartoris, R. Baggio, M. T. Garland, and M. Perec, Inorg. Chem. **47**, 10389 (2008).
[13] K. P. Schmidt, and G. S. Uhrig, Phys. Rev. Lett. **90**, 227204 (2003).
[14] A. W. Overhauser, Phys. Rev. **101**, 1702 (1956).
[15] H. Sternlicht, and H. M. McConnell, J. Chem. Phys. **35**, 1793 (1961); H. M. McConnell and R. M. Lynden-Bell, *ibid*. **36**, 2393 (1962).
[16] R. M. Lynden-Bell, and H. M. McConnell, J. Chem. Phys. **37**, 794 (1962).
[17] P. L. Nordio, Z. G. Soos, and H. M. McConnell, Ann. Rev. Phys. Chem. **17**, 237 (1966).
[18] S. Sachdev, and R. N. Bhatt, Phys. Rev. B **41**, 9323 (1990).
[19] T. Giamarchi, and A. M. Tsvelik, Phys. Rev. B **59**, 11398 (1999).
[20] B. Kumar, Phys. Rev. B **82**, 054404 (2010).
[21] M. Matsumoto, B. Normand, T. M. Rice, and M. Sigrist, Phys. Rev. Lett. **89**, 077203 (2002); Phys. Rev. B **69**, 054423 (2004).
[22] M. Matsumoto, T. Shoji, and M. Koga, J. Phys. Soc. Jpn. **77**, 074712 (2008); A. A. Aczel, Y. Kohama, C. Marcenat, F. Weickert, M. Jaime, O. E. Ayala-Valenzuela, R. D. McDonald, S. D. Selesnik, H. A. Dabkowska, and G. M. Luke, Phys. Rev. Lett. **103**, 207203 (2009).
[23] S. Sachdev, Nature Physics **4**, 173 (2008).
[24] S. Sachdev, *Quantum Phase Transitions* (Cambridge University Press, Cambridge, 2001).
[25] A. Oosawa, M. Ishii, and H. Tanaka, J. Phys. Condens. Matter **11**, 265 (1999).
[26] T. Nikuni, M. Oshikawa, A. Oosawa, and H. Tanaka, Phys. Rev. Lett. **84**, 5868 (2000).
[27] T. M. Rice, Science **298**, 760 (2002).
[28] E. Ruiz, S. Alvarez, A. Rodríguez-Fortea, P. Alemany, Y. Pouillon, and C. Massobrio, in *Magnetism: Molecules to Materials II. Molecule based materials*, edited by J. S. Miller and M. Drillon (Wiley-VCH, Weinheim, 2001), p. 227.
[29] N. Cavadini, G. Heigold, W. Henggeler, A. Furrer, H.-U. Güdel, K. Krämer, and H. Mutka, Phys. Rev. B **63**, 172414 (2001).
[30] A. Oosawa, M. Fujisawa, T. Osakabe, K. Kakurai, and H. Tanaka, J. Phys. Soc. Jpn. **72**, 1026 (2003); C. Rüegg, Nature **423**, 62 (2003); C. Rüegg, A. Furrer, D. Sheptyakov, T. Strässle, K. W. Krämer, H.-U. Güdel, and L. Mélési, Phys. Rev. Lett. **93**, 257201 (2004); C. Rüegg, B. Normand, M. Matsumoto, C. Niedermayer, A. Furrer, K. W. Krämer, H.-U. Güdel, P. Bourges, Y. Sidis, and H. Mutka,

ibid. **95**, 267201 (2005); C. Rüegg, B. Normand, M. Matsumoto, A. Furrer, D. F. McMorrow, K. W. Krämer, H.-U. Güdel, S. N. Gvasaliya, H. Mutka, and M. Boehm, *ibid*. **100**, 205701 (2008).

[31]M. Jaime, V. F. Correa, N. Harrison, C. D. Batista, N. Kawashima, Y. Kazuma, G. A. Jorge, R. Stern, I. Heinmaa, S. A. Zvyagin, Y. Sasago, and K. Uchinokura, Phys. Rev. Lett. **93**, 087203 (2004); S. E. Sebastian, D. Yin, P. Tanedo, G. A. Jorge, N. Harrison, M. Jaime, Y. Mozharivskyj, G. Miller, J. Krzystek, S. A. Zvyagin, and I. R. Fisher, Phys. Rev. B **71**, 212405 (2005); N. Harrison, S. E. Sebastian, C. D. Batista, M. Jaime, L. Balicas, P. A. Sharma, N. Kawashima, and I. R. Fisher, J. Phys. Conf. Series **51**, 9 (2006).

[32]S. E. Sebastian, P. A. Sharma, M. Jaime, N. Harrison, V. Correa, L. Balicas, N. Kawashima, C. D. Batista, and I. R. Fisher, Phys. Rev. B **72**, 100404 (2005).

[33]S. E. Sebastian, N. Harrison, C. D. Batista, L. Balicas, M. Jaime, P. A. Sharma, N. Kawashima, and I. R. Fisher, Nature **441**, 617 (2006).

[34]S. E. Sebastian, P. Tanedo, P. A. Goddard, S. C. Lee, A. Wilson, S. Kim, S. Cox, R. D. McDonald, S. Hill, N. Harrison, C. D. Batista, and I. R. Fisher, Phys. Rev. B **74**, 180401 (2006).

[35]S. A. Zvyagin, J. Wosnitza, J. Krzystek, R. Stern, M. Jaime, Y. Sasago, and K. Uchinokura, Phys. Rev. B **73**, 094446 (2006).

[36]C. J. Gorter and J. H. VanVleck, Phys. Rev. **72**, 1128 (1947).

[37]J. H. Van Vleck, Phys. Rev. **74**, 1168 (1948).

[38]P. W. Anderson, and P. R. Weiss, Rev. Mod. Phys. **25**, 269 (1953).

[39]P. W. Anderson, J. Phys. Soc. Jpn. **9**, 316 (1954).

[40]R. Kubo and K. Tomita, J. Phys. Soc. Jpn. **9**, 888 (1954).

[41]R. Kubo, in *Stochastic Processes in Chemical Physics, Advances in Chemical Physics*, edited by K. E. Schuler (Wiley, New York, 1969), Vol. XV, p. 101.

[42]R. Kubo, M. Toda, and N. Hashitsume, *Statistical Physics II. Nonequilibrium Statistical Mechanics* (Springer, Berlin, 1978).

[43]P. W. Anderson, Phys. Rev. **109**, 1492 (1958); N. V. Prokof'ev and P. C. E. Stamp, Rep. Prog. Phys. **63**, 669 (2000).

[44]D. M. Martino, M. C. G. Passeggi, and R. Calvo, Phys. Rev. B **52**, 9466 (1995); D. M. Martino, M. C. G. Passeggi, R. Calvo, and O. R. Nascimento, Physica B **225**, 63 (1996).

[45]A. J. Costa-Filho, C. E. Munte, C. Barberato, E. E. Castellano, M. P. D. Mattioli, R. Calvo, and O. R. Nascimento, Inorg. Chem. **38**, 4413 (1999); A. J. Costa-Filho, O. R. Nascimento, L. Ghivelder, and R. Calvo, J. Phys. Chem. B **105**, 5039 (2001); A. J. Costa-Filho, O. R. Nascimento, and R. Calvo, *ibid*. **108**, 9549 (2004); R. C. Santana, R. O. Cunha, J. F. Carvalho, I. Vencato, and R. Calvo, J. Inorg. Biochem. **99**, 415 (2005); E. F. Chagas, R. E. Rapp, D. E. Rodrigues, N. M. C. Casado, and R. Calvo, J. Phys. Chem. B **110**, 8052 (2006); E. D. Vieira, N. M. C. Casado, G. Facchin, M. H. Torre, A. J. Costa-Filho, and R. Calvo, Inorg. Chem. **45**, 2942 (2006); E. D. Vieira, G. Facchin, M. H. Torre, and A. J. Costa-Filho, J. Braz. Chem. Soc. **19**, 1614 (2008).

[46]R. Calvo, Appl. Magn. Reson. **31**, 271 (2007).

[47]H. M. Pastawski, Physica B **398**, 278 (2007); A. D. Dente, R. A. Bustos-Marún, and H. M. Pastawski, Phys. Rev. A **78**, 062116 (2008).

[48]R. Calvo, E. C. Abresch, R. Bittl, G. Feher, W. Hofbauer, R. A. Isaacson, W. Lubitz, M. Y. Okamura, and M. L. Paddock, J. Am. Chem. Soc. **122**, 7327 (2000); R. Calvo, R. A. Isaacson, M. L. Paddock, E. C. Abresch, M. Y. Okamura, A. L. Maniero, L. C. Brunel, and G. Feher, J. Phys. Chem. B **105**, 4053 (2001).

[49]W. Wernsdorfer, N. Aliaga-Alcalde, D. N. Hendrickson, and G. Christou, Nature **416**, 406 (2002); W. Wernsdorfer, S. Bhaduri, R. Tiron, D. N. Hendrickson, and G. Christou, Phys. Rev. Lett. **89**, 197201 (2002).

[50]E. Wasserman, L. C. Snyder, and W. A. Yager, J. Chem. Phys. **41**, 1763 (1964).

[51]J. R. Wasson, C.-I. Shyr, and C. Trapp, Inorg. Chem. **7**, 469 (1968).

[52]J. S. Valentine, A. J. Siverstein, and Z. G. Soos, J. Am. Chem. Soc. **96**, 97 (1974).

[53]L. M. B. Napolitano, O. R. Nascimento, S. Cabaleiro, J. Castro, and R. Calvo, Phys. Rev. B **77**, 214423 (2008).

[54]M. Perec, R. Baggio, R. P. Sartoris, R. C. Santana, O. Peña, and R. Calvo, Inorg. Chem. **49**, 695 (2010).

[55]N. I. Neuman, M. Perec, P. J. Gonzalez, M. C. G. Passeggi, A. C. Rizzi, and C. D. Brondino, J. Phys. Chem. A **114**, 13069 (2010).

[56]O. R. Nascimento, L. M. B. Napolitano, M. H. Torre, O. Peña, and R. Calvo, J. Braz. Chem. Soc. **22**, 669 (2011).

[57]T. Tokii, N. Watanabe, M. Nakashima, Y. Muto, M. Morooka, S. Ohba, and I. Saito, Bull. Chem. Soc. Jpn. **63**, 364 (1990).

[58]A. M. Gennaro, P. R. Levstein, C. A. Steren, and R. Calvo, Chem. Phys. **111**, 431 (1987); C. D. Brondino, N. M. C. Casado, M. C. G. Passeggi, and R. Calvo, **32**, 2078 (1993).

[59]S. Stoll and A. Schweiger, J. Magn. Reson. **178**, 42 (2006).

[60]MatLab, *The MathWorks, Inc*. (Natick, MA, 2002).

[61]Y. Servant, J. C. Bissey, and M. Maini, Physica B **106**, 343 (1981); R. Calvo, M. A. Mesa, G. Oliva, J. Zukerman-Schpector, O. R. Nascimento, M. Tovar, and R. Arce, J. Chem. Phys. **81**, 4584 (1984); R. Calvo, P. R. Levstein, E. E. Castellano, S. M. Fabiane, O. E. Piro, and S. B. Oseroff, Inorg. Chem. **30**, 216 (1991).

[62]A. Ozarowski, Inorg. Chem. **47**, 9760 (2008).

[63]N. D. Chasteen, Inorg. Chem. **10**, 2339 (1971); B. Kozlevĉar, I. Leban, M. Petriĉ, S. Petriĉek, O. Roubeau, J. Reedijk, and P. Šegedin, Inorg. Chim. Acta **357**, 4220 (2004); J. Lopes de Miranda, J. Felcman, M. H. Herbst, and N. V. Vugman, Inorg. Chem. Comm. **11**, 655 (2008).

[64]M. C. G. Passeggi, and R. Calvo, J. Magn. Reson. Ser. A **114**, 1 (1995).

[65]F. Carboni, and P. M. Richards, Phys. Rev. **177**, 889 (1969); R. Calvo and M. C. G. Passeggi, **44**, 5111 (1991).

[66]R. Calvo, H. Isern, and M. A. Mesa, Chem. Phys. **100**, 89 (1985).

[67]Z. G. Soos, J. Chem. Phys. **44**, 1729 (1966).

[68]S. A. Zvyagin, J. Wosnitza, J. Krzystek, R. Stern, M. Jaime, Y. Sasago, and K. Uchinokura, J. Magn. Magn. Mater **310**, 1206 (2007).

[69]J.-M. Lehn, *Supramolecular Chemistry. Concepts and perspectives* (VCH, Weinheim, 1995).

[70]S. Grimme, Angew. Chem. Int. Ed. **47**, 3430 (2008).

[71]C. D. Brondino, R. Calvo, A. M. Atria, E. Spodine, and O. Peña, Inorg. Chim. Acta **228**, 261 (1995).